Journal of Bio- and Tribo-Corrosion (2019) 5:96
https://doi.org/10.1007/s40735-019-0284-y

Optimization and Analysis of Wear Rate of CFRP-NanoZno/Nanoclay Hybrid Composites Using RSM

Vipin Kumar Tripathi[1] · Shailesh Ambekar[1]

Received: 12 April 2019 / Revised: 14 August 2019 / Accepted: 10 September 2019 / Published online: 23 September 2019

Abstract
The aim of the current work is to do an experimental study and investigation of the sliding wear behavior of carbon fiber reinforced polymer (CFRP) hybrid nano composite with montmorillonite nanoclay and nanoZnO as fillers. The wear properties of CFRP hybrid nanocomposites were tested by using a pin-on-disc machine under various loads. Optimization of the wear rate of CFRP hybrid nanocomposites was carried out by using the central composite design method, subset of the response surface methodology. The mathematical model predicts the significance of the independent variables, i.e., wt% of nanoZnO, nanoclay, and fiber orientation angle on the wear rate of CFRP hybrid nanocomposites. The lowest value obtained for wear rate was 2.22 mg/Nm which appeared when actual values were nanoclay = 3 %wt, nanoZnO = 3 %wt, and fiber orientation = 45°, respectively. The results of optimization also showed that the wear rate at the optimum value was much improved or minimized by about 3 times than that of the controlled sample. From the SEM micrographs, surface readings also show the effective improvement in the wear resistance in CFRP with the addition of nanoparticles.

Keywords Hybrid nano composites · Nanoclay · NanoZnO · Wear rate · RSM

1 Introduction

In modern decades, fiber-reinforced polymers are powerfully used in tribological elements such as cams, brakes, bearings, gears, etc., because of their improved wear resistance and a capability of self-lubrication. Polymer composites have a superior strength-to-weight ratio, which is useful in a range of applications in automobiles, aerospace, and various household appliances [3.9]. The deficiency of fiber-reinforced polymer (FRP) composites can be defeat productively by using various fillers like nano- or micro-sized particles. The effects of the addition of nanoparticles on these properties have been broadly studied and its usefulness is proved by the various researchers. The adding up of a few percent of nanoparticles by weight results in a major development in the mechanical properties [1–9].

✉ Shailesh Ambekar
sd.ambekar@gmail.com

Vipin Kumar Tripathi
vkt.mech@coep.ac.in

[1] Department of Mechanical Engineering, College of Engineering, Shivajinagar, Pune 411005, India

The FRP composites always got a high mechanical performance because of fiber as a most effective reinforcement [12, 14]. It is found that carbon fiber reinforced composites have better properties such as enhanced thermal conductivity, better strength, higher Young's modulus, and brilliant electrical properties [9–12]. By the use of inorganic nanoparticles, one can improve toughness, stiffness, other friction, and wear properties of FRP composites [1–3] and Deca et al. found that there is an enhancement in the Ultraviolet rays (UV) resistance and thermal stability of the polymers of wood with the incorporation of nanoZnO and nanoclay [4]. Rashmi et al. and Li Chang et al. studied the improvement in the wear resistance for short/regular-sized CFRP composites with the nanoparticles effect [5, 6]. As mentioned by Shazed et al., the carbon nanotubes are also supportive in convalescing the tensile and mechanical properties of carbon fibers with different fiber orientations [7]. David et al. derived that fracture toughness can be significantly improved by effect of the nanoparticles in the CFRP composites [8]. With the addition of fillers such as carbon nanotubes (CNTs), nanoZnO results in astonishing mechanical, electrical, and thermal properties of the host matrix/composite materials [9, 10].

As per research, there is enhancement in wear resistance and mechanical properties of polyester woven carbon fiber,

jute fiber, and chopped carbon fiber with the additional effect of nanoZnO [11–13]. By using surface-grown hydrothermal ZnO, nanorods can be used to enhance the vibration damping of FRP as per Alipour et al. [14]. The characterization processing of ZnO-incorporated polymer composites are confirmed by Chuangqi et al. and Kyungil Kong et al. [12, 15]. Yasser Rostamiyan et al. have found that there is an improvement in the flexural strength, tensile, and impact strength up to considerable higher amount of the glass fiber-reinforced composite with addition of nanoclay as filler used in epoxy resin [16, 17]. Tripathi et al. have derived a method for optimal design of a FRP laminate by taking into account different parameters like ply angle, ply thickness, and focused on a procedure to get optimum composition of the friction liners material [18, 19]. The studies are carried out by using the RSM for the design of experiments. Sanes et al. [20] found that using ZnO nanoparticles as a filler increases the stiffness and the chain mobility enhances because of the IL phase addition which results in a plasticizing effect. Also, the friction coefficient gets reduced by 50% and the rate of wear by a considerable order of magnitude because of the IL lubricant effect. Bahadur et al. [21] focused on the wear characteristics of polyphenylene sulfide (PPS) added with inorganic nanoparticles like ZnO, CuO, TiO_2, and SiC. Yingke et al. have premeditated the tribological behavior of nanosilica coating on epoxy resin composite, and coating composition on the wear and friction behavior illustrated in relation with their microstructure [22].

Friction and wear properties of aligned carbon nanotube filled epoxy composites and short carbon fibers polyimide composites filled with microSiO_2 and graphite were studied by Lei Yan et al. in their respective studies [23, 24]. Aluminum composites give an improved wear resistance and hardness with a filling of ZrO_2 particles in an aluminum matrix as per the findings of Ramachandra et al. [25]. Shadpour et al. highlighted the ZnO filler effect on the morphology, thermal conductivity, and various properties of polymer nanocomposites [26]. Zhang et al. also expressed that nanoparticles as a filler results in reduction of the wear rate and friction significantly, and they can entail an improved tribological performance than the sub-micron particles [27]. Rajasekhar et al. presented their work on tribological behavior of Polyamide Jute Fiber filled with nanoZnO and found that both, the wear rate and friction coefficient of the nanocomposites, were lowered significantly than pure polyamide [13]. Sudeepan et al. studied friction/wear of polymer composite of ABS/ZnO by using the Taguchi method and found that the specific wear rate and friction coefficient are influenced by the increase of load, speed, and filler content [28]. Zhao et al. have focused on the micro/nanoparticles effect on the wear and friction properties of CFRP [29]. Senthil Kumar et al. have done a tribological analysis of nanoclay, epoxy, and glass fiber by using Taguchi's technique [30]. Many researchers have focused on the effect of CNT/other nanoparticles on PEEK and other nanocomposites [31–34]. Shailesh Ambekar et al. successfully incorporated the use of nanoclay and nanoZnO for the enhancement and optimization of the CFRP flexural strength [35]. Zhou et al. have developed the fracture-based model to predict the wear damage due to chipping, the model was able to predict the size of the wear particles [36]. Liu, Zhou, and Wang et al. have focused their study on modeling and properties of 2D graphene nanoparticles and grain size effect on the mechanical properties of nanocrystalline carbon, respectively [37, 38] As before stated in literature review, the dry and sliding wear behavior of CFRP incorporated with hybrid combination of clay and NanoZnO is not studied till date. So, in the current study, the focus is on the experimental exploration of the influence of nanoparticles like nanoZnO, fiber angle, and nanoclay on the wear behavior of CFRP polymer composites. The new material, i.e., CFRP hybrid nanocomposites with incorporation of nanoclay and nanoZnO can be used in carbon–carbon disc brakes, friction clutches, various parts of the space craft, aeroplanes, and automotive gear box which nowadays are being used in racing cars and in fabrication of automobile variable transmission systems from these CFRP hybrid nanocomposites. The fiber orientation angle, wt % of nanoZnO and wt % of nanoclay montmorillonite nanoclay are chosen as independent variables and the wear rate performance carbon fiber reinforced polymers with the mixture of nanoclay and nanoZnO, new material system is derived with the application of fiber orientation angle as third variable their effect of on the rate of wear hybrid CFRP composite laminate has been investigated by using CCD in RSM. Central composite design (CCD) is the part of response surface design methodology that has been used to derive models as a function in terms of factors to forecast the wear rate of the newly fabricated CFRP hybrid nanocomposite. It has also been used to derive a mathematical model so as to develop the optimum design or structure of a new CFRP hybrid nanocomposite. The total 20 experiments were designed including six center point replicates as per the MATLAB. Accordingly, the samples were prepared and tested for wear rate of the CFRP hybrid nanocomposites with different fiber orientation angles and nanoclay, nanoZnO particles as filler.

2 Materials and Experimental Characterization

2.1 Materials

In the current study, Control sample was carbon fiber reinforced (CFRP) composites. The carbon fiber of 200 GSM, standard modulus of 3 K, and HCU200 code are used for the main reinforcement. Hinpoxy C epoxy resin is bisphenol-A-based liquid-state material. HARDENER-B is a modified amine hardener, low viscosity, colorless liquid, with stoichiometric ratio of A:B = 10:3; the carbon fiber and the resin both were supplied by the Hindoostan Mills Ltd. Mumbai, India. Nano zinc oxide (ZnO) particles and montmorillonite nanoclay were used, supplied by Nano Research Lab. Jamshedpur, (Jharkhand), India. All the details of the properties are as given in Table 1.

2.2 Sample Fabrication

The CFRP nanocomposite laminates were manufactured by a hand layup method (as shown in Fig. 1a), succeeded by vacuum bagging the unidirectional carbon fiber was the main part of the reinforcement in the epoxy resin. Bisphenol A (DGEBA) resin was mixed with a hardener at a ratio of 100:30 by weight. The clay and Zinc Oxide nanoparticles were used as filler. For the suitable dispersion in the epoxy resin clay and Zinc Oxide nanoparticles, nanoparticles were dried prior to use for overnight at 75 °C in an oven. For attainment of a uniform dispersion of the Montmorillonite nanoclay and Zinc Oxide nanoparticles in the epoxy resin, magnetic stirring (as shown in Fig. 1b) and ultrasonication (as shown in Fig. 1c) were done for better mixing. The %wt of nanoparticle content was used in the range 1 to 5 %wt with the epoxy resin and hardener mixture as per the results from OVAT analysis and previous research carried out. Ultra-sonic method was then carried out for 40 min at 40° C for uniform mixing of the nanoparticles in the epoxy resin. After ultrasonication, the said mixture was magnetically stirred for one and a half hour. The prepared mixture was then used for the composite preparation. The hand layup Fig.1(c) and vacuum bagging process (as shown in Fig. 1d) are used for the preparation test sample, the process of vacuum bagging is carried out for 4.5–5 h with application of constant vacuum pr. of 720 mm Hg. Fourteen plies were used and according to the coded levels, the combination of three factors was varied. The specimen was kept within the bag for 15–18 h at room temperature for curing. The post curing of specimen was then done in an oven for 5 h at 80 °C. Then the round specimens were cut from the laminates as per the required dimensions for wear test.

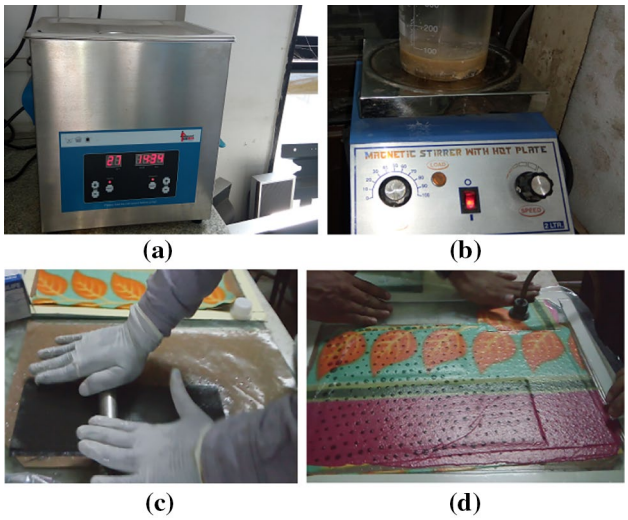

Fig. 1 **a** Ultrasonication, **b** Magnetic stirring, **c** Hand Lay up of CFRP, **d** Vacuum bagging

Table 1 Material properties

Properties of carbon fiber	
Properties	Value
Density (g/cm^3)	1.8
Tensile strength (MPa)	4000
Elongation (%)	1.7
Filament diameter (μm)	7
Tensile modulus (GPa)	240
Properties—Hinpoxy C resin	
Viscosity at 25 °C, mPas	9000–12,000
Density at 25 °C, g/cc	1.15–1.20
Flash point, °X	> 200
Properties—Hinpoxy C hardener	
Viscosity at 25 °C, mPas	< 50
Density at 25 °C, g/cc	0.94–0.95
Flash point, °X	>123
NanoZno properties	
Purity	99.9%.
SSA	20–60 m^2/g
Morphology	Nearly spherical
True density	6 g/cm^3
Average particles size	30–50 nm
Color	Milky white
Bulk density	0.28–0.48 g/cm^3
Nanoclay properties	
Purity	99.9%.
Stack size	5–10 μm
Bulk density	37 to 56 lbs./ft3

2.3 Experimental Procedure

For the wear test, a pin-on-disc tribo tester experimental setup, DUCOM, made in Bangalore was used to test the

wear behavior of CFRP hybrid nanocomposite according to the ASTM G99 standard. The dry and sliding wear behavior was tested in the performed experiments The disc setup that was used was made from an alloy steel with 8 mm thickness and 165 mm diameter and of 62 HRC hardness. A surface specimen of size 10 mm in diameter and 3 mm thick was glued at the end of the pin of the mild steel. The total height of the specimen pin along with the sample piece was around 28 mm. Before start of the test, the disc was use to cleaned with acetone. The specimen was positioned in its holder normal to the steel disc. For each individual specimen, three trials were conducted on the pin-on-disc test setup and average reading values were used. Tests performed for the sample combinations as per the coded values given in Table 3. The weight of the pin assembly with the specimen was measured in an electronic balance of accuracy 0.0001 g. The weight loss was determined from initial wt and final wt after wear test of the specimen was recorded. The wear rate can be calculated from the ratio of weight loss and product of the sliding distance and the normal load by using Eq. 1. The coefficient of friction was taken directly from the setup. The wear rate was calculated for three different weights; 10 N, 15 N, and 20 N and the sliding velocity was at 2.09 m/s. According to the Archard equation, the model considers adhesive wear and assumes the sliding spherical asperities to deform fully plastically in contact. The area of contact then is circular with the contact area equal to πa^2, where a is the radius. After the asperity slides, a distance of it is released from the contact and there is a probability K. The mean contact pressure in this case equals to hardness of the softer material, and thus $= P/\pi a^2$. Then the wear volume per sliding distance $2a$, $W = K\pi a^2/3$, $\pi a^2 = P/H \times W = P \times K/3H = k \times P/H$.

$$V_T = W \times s = k \times P/H,$$

$$V_T/A = W \times s = k \times P/A/H$$

$$\text{Wear rate} = \frac{\text{weight loss}}{\text{normal load}} \times \text{sliding distance}$$

$$WR = \frac{w}{Fn \times L} \tag{1}$$

Experimental conditions	
Parameters	Operating conditions
Temperature	Ambient conditions (temperature: 29° C)
Relative humidity	55(±5) %
Test disc	Hardened ground steel (EN-31, hardness 60 HRC

Experimental conditions	
Parameters	Operating conditions
Roughness of EN-31	1.6 m Ra
Duration of rubbing	600 s
Surface condition	Dry
Load	10 N, 15 N, 20 N
Sliding speed	2.09 m/s
Sliding distance	1500 m
Pin size (ASTM G99 Std.)	30 mm × 10 mm × 10 mm
The average contact pressure between the disc and specimen surface	0.3 MPa

2.4 Design of Experiments

The design of experiments was carried out by Response surface methodology (RSM), which is a mathematical and statistical technique of data collection. This technique is useful for design of experiments, to evaluate the effect of independent variables on final response, optimizing the processes and model building. In recent years, RSM has played important role in various fields of chemistry, biotechnology, nanotechnology, etc. It is important capability of RSM that it can develop quite true relationship function between the set of independent variables and response (Y) and following is the first-order model polynomial equation, which is used to describe a linear function between independent variables and response (Fig. 2).

$$Y = \beta_0 + \beta_1 X_1 + \beta_2 X_2 + \cdots \cdots \cdots \cdots +_k X_k \tag{2}$$

where the independent variables are X_1, $X_2 \ldots X_k$ and β_k is the linear of the K_{th} coefficient factor, β_0 is the constant coefficient, and ε is the error observed. If there is curve in the

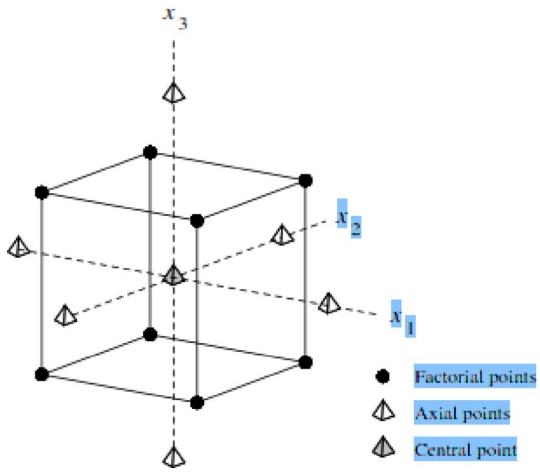

Fig. 2 Central composite design for three design variables at two levels

system, then the second-order polynomial model should be used. This model will take the form

$$Y = \beta_0 + \sum_{i=1}^{k} \beta_i X_i + \sum_{i=1}^{k} \beta_{ii} X_i^2 + \sum_{i<j} \beta_{ij} X_i X_j + \varepsilon \quad (3)$$

2.4.1 Central Composites Design

Central composite design is RSM part set, which helps in design for fitting second-order models. The total experiment count for CCD is equal to $2^k + 2k + \eta_0$, where 2^k is the number of standard two-level factorial points, k is the number of design factors, 2k points are the star points which are located at "$\pm\alpha$" from the center points of the domain of experiment, and the center point is η_0 of domain which is to be replicated to estimate the "pure" experimental variance error. When the variance of variables is constant at all distances from the center point then the design is named as Rotatable central composite design named CCRD. Rotatability can be calculated from the equation given below

$$\alpha = \left(2^k\right)^{1/4} \quad (4)$$

For statistical calculation, X_i (experimental variables) has been coded as x_i with the following transformation.

$$X_i = \frac{X_i - X_0}{\Delta X_0} \quad (5)$$

here x_i is coded the dimensionless value of the i^{th} variable of experiment, X_i stands for uncoded independent i^{th} variable, X_0 stands for the magnitude of X_i situated at center point, and ΔX_i indicates the step change value for the real variable i.

In this experimental study, the Minitab software was used to analyze the data evaluation and to get results using CCD as methodology for experimental design. Here, nanoZnO wt%, fiber angle in degrees were used as inputs and the response was wear rate. Total 20 experimental levels for

Table 2 Actual and coded level of design parameter

Factors	Levels			Star point $\alpha = 1.68179$	Star point $\alpha = -1.68179$
	Low (−1)	Center (0)	High (+1)	−α	+α
(A) Content of clay (wt%)	1.8	3	4.2	1	5
(B) Content of ZnO (wt%)	1.8	3	4.2	1	5
(C) Fiber angle	18.2°	45°	71.2°	0°	90°

Table 3 Coded and actual values of factors

Code Sr. no	Coded value A	Coded value B	Coded value C	Weight loss (mg)	Wear rate (g/Nm)
1	1.681793	0	0	1.563	1.3028
2	0	0	− 1.68179	0.319	0.2657
3	− 1.68179	0	0	0.830	0.6917
4	− 1	1	1	0.546	0.4546
5	1	1	1	0.937	0.7806
6	− 1	− 1	− 1	0.526	0.4380
7	1	1	− 1	0.907	0.7556
8	− 1	1	− 1	0.676	0.5630
9	1	− 1	− 1	0.796	0.6630
10	0	0	0	0.503	0.4194
11	0	0	0	0.267	0.2222
12	0	0	0	0.306	0.2546
13	0	− 1.68179	0	0.621	0.5176
14	0	1.681793	0	0.373	0.3111
15	0	0	0	0.433	0.3611
16	1	− 1	1	1.090	0.9083
17	0	0	1.681793	0.707	0.5889
18	0	0	0	0.481	0.4009
19	− 1	− 1	1	0.666	0.5546
20	0	0	0	0.314	0.2620

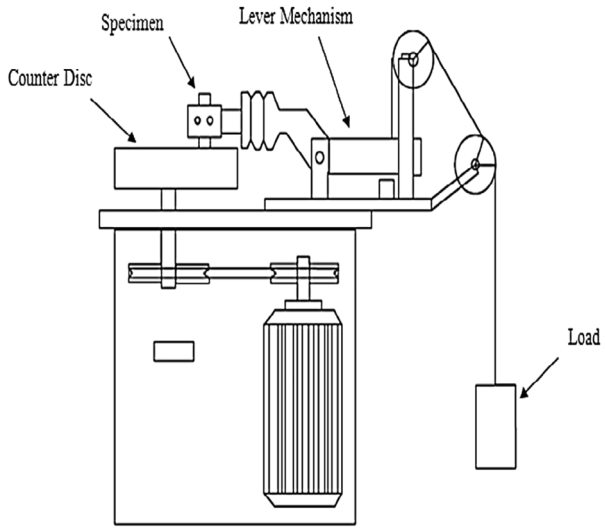

Fig. 3 Schematic diagram of pin-on-disc wear test setup

three factors were designed and at the center point with six replicates. Tables 2 and 3 show coded level and actual level of the design parameter and experiments generated and the corresponding wear rate for each test (Fig. 3).

In this experiment, the software of Minitab was used to interpret and analyze the data processing and to obtain results, and for the design of experiments CCD was chosen. Here, the input variables were nanoZnO wt%, nanoclay wt%, and fiber orientation angle and the response was the weight loss or wear rate. A total of 20 experimental levels were designed for three factors with six replicates at the center point. Tables 2 and 3 show the coded level and actual level of the design parameter, the experiments generated, and the corresponding wear results for each test.

3 Results and Analysis

As the input variables are nanoclay wt%, nanoZnO wt%, and fiber orientation angle which are denoted as A, B, and C, respectively, in analysis of variance, the response was wear rate of CFRP filled with nanoclay and nanoZnO. In this step, to evaluate the influence of these independent variables on corresponding response, analysis of variance was carried out by Minitab software according to the model of CCD and results determined based on considering the confidence level equals to 95% ($\alpha = 0.05$). According to probability, P value significance of each term was evaluated. The probability value more than 95% ($\alpha \leq 0.05$) should be possessed by the significant terms.

3.1 Analysis of Variance and Fitting Regression Model

The ANOVA results of the analyses were as shown in Table 4. As seen, the fiber orientation nano and clay wt% angle had a significant value of P, probability greater than 95%. The wt% of nanoZnO was not significant probability, with a value less than 95% on the wear rate. From Table 4, it can also be seen that square values of the nanoclay wt% and fiber angle/orientation were most effective having a probability value of $P \geq 95\%$. With a probability value less than 95% from the square of nanoZnO, the wt% had no significant effect. It was observed that the interaction between nanoZnO and fiber orientation is the main interaction with good effective probability value. With a P value of about 0.552, an insignificant "lack of fit" indicates that the data satisfactorily fitted for the model; therefore the CCD was a best choice for the experiment design and the analysis of the results.

Regression Equation in uncoded units response surface regression: Wear rate (Y) versus A, B, C (nanoclay wt%, nanoZnO wt%, Fiber orientation angle)

$$Y = 0.3198 + 0.1556A - 0.0262B + 0.0602C + 0.2413A^2 + 0.0352B^2 + 0.0398C^2 - 0.0075AB + 0.0328AC - 0.0557BC \quad \text{For initial analysis}$$

$$Y = 0.3486 + 0.1556A - 0.0262B + 0.0602C + 0.2378A \times A + 0.0363C \times C - 0.0557B \times C \quad \text{For final analysis}$$

For the final analysis, the analysis process was then repeated by eliminating terms which were non-effective and the ANOVA results are displayed in Table 5. It is obvious that the P value of the significant terms and also the ''Lack of Fit'' magnitude increased after eliminating the insignificant terms. The above equation shows the reduced fitted model after eliminating the insignificant terms. Table 5 indicates the regression coefficients of the three independent variables, squares and interaction between factors.

Moreover, Tables 6 shows the determination coefficient (R^2) which is generated for ability of evaluation of the model in predicting the results, when this value is close to a 100%, it is capable to give more accurate results. The values of R^2 were 95.01 and 92.99% for the first one overall model and the successor reduced model, respectively. These higher R^2 values indicated that the model repressors could not explain only about 6% of the total variable values. The derived regression model is enabled for a good evaluation of response for the studied range.

Figure 4a and b displays the normal residuals probability plot for the initial and final analysis. These plots resolved by comparing different sample distributions, whether a particular distribution fits or not for the collected data. The two sections of this figure show that the closeness of points to the

Table 4 Initial analysis of variance

Source	DF	Adj SS	Adj MS	*F* value	*P* value
Model	9	1.26755	0.140838	21.16	0.000
Linear	3	0.38950	0.129832	19.51	0.000
A	1	0.33064	0.330644	49.68	0.000
B	1	0.00936	0.009355	1.41	0.263
C	1	0.04950	0.049497	7.44	0.003
Square	3	0.84422	0.281407	42.28	0.000
A × A	1	0.83914	0.839142	126.09	0.000
B × B	1	0.01789	0.017886	2.69	0.004
C × C	1	0.02284	0.022842	3.43	0.132
2-Way interaction	3	0.03383	0.011277	1.69	0.0231
A × B	1	0.00045	0.000453	0.07	0.800
A × C	1	0.00858	0.008583	1.29	0.283
B × C	1	0.02479	0.024794	3.73	0.082
Error	10	0.06655	0.006655		
Lack-of-fit	5	0.03123	0.006246	0.88	0.552
Pure error	5	0.03532	0.007064		
Total	19	1.33410			

Model summary

S	R^2	R^2(adj)	R^2(pred)
0.0815799	95.01%	90.52%	78.41%

DF The total degrees of freedom are the amount of information in your data. The analysis uses the information to estimate the values of unknown population parameters. The total DF is determined by the number of observations in your sample. The DF for a term shows how much information that term uses. Increasing your sample size provides more information about the population, which increases the total DF. Increasing the number of terms in your model uses more information, which decreases the DF available to estimate the variability of the parameter estimates, *Adj SS* adjusted sums of squares are measures of variation for different parts of the model, *Adj MS* adjusted mean squares measure how much variation a term or a model explains, assuming that all other terms are in the model, *F value* is the test statistic used to determine whether any term in the model is associated with the response, including blocks and factor terms, *P value* the *p* value is a probability that measures the evidence against the null hypothesis. Lower probabilities provide stronger evidence against the null hypothesis, *S* represents the standard deviation of the distance between the data values and the fitted values. *S* is measured in the units of the response, *R-sq* R^2 is the percentage of variation in the response that is explained by the model. It is calculated as 1 minus the ratio of the error sum of squares (which is the variation that is not explained by model) to the total sum of squares (which is the total variation in the model), *R-sq(adj)* adjusted R^2 is the percentage of the variation in the response that is explained by the model, adjusted for the number of predictors in the model relative to the number of observations. Adjusted R^2 is calculated as 1 minus the ratio of the mean square error (MSE) to the mean square total (MS Total), *R-sq(pred)* predicted R^2 is calculated with a formula that is equivalent to systematically removing each observation from the data set, estimating the regression equation, and determining how well the model predicts the removed observation. The value of predicted R^2 ranges between 0 and 100%

fitted distribution line, in both analyses, but it can be seen that the points for the final analysis fall closer to the distribution line than the points fitted for the initial one. So, for both the models, the distribution of the wear rate was close to normal distribution. The plot of residuals versus the fitted values for the initial and the final analysis of variance as shown in Fig. 5a and b indicate that the residuals on the plot scattered randomly for both the analyses. However, it can be observed that the tendency of the scattering in the first stage of analysis is much superior than the further one. Hence, it is found that the model proposed was satisfactory. Figure 6 shows the main effects plot of the variable inputs. This plot gives the significance of linear terms on the response and shows that the amount of the wear rate decreased with an increase in the nanoclay wt% from 1 to 2 wt%. The wear rate increased when the nanoclay wt% was between 3 and 4.2%. The effect of the nanoZnO can be seen and it shows that the wear rate decreased when the wt% of the ZnO was between 1 and 1.8%. The wear rate increased from 1.8 to 3% and then a decreasing trend was followed by the wear rate from 3% onwards. A similar kind of fashion trend is observed in the outcome of fiber orientation angle effect on the wear rate in the third part of the figure. From this, it can be consummated that all the results were in conformity with what was observed in the ANOVA tables and also an signal of the fitted regression coefficients.

Table 5 Final analysis of variance

Source	DF	Adj SS	Adj MS	*F* value	*P* value
Model	9	1.24062	0.206771	28.76	0.000
Linear	3	0.38950	0.129832	18.06	0.000
A	1	0.33064	0.330644	45.98	0.000
B	1	0.00936	0.009355	1.30	0.275
C	1	0.04950	0.049497	6.88	0.003
Square	3	0.82633	0.413167	57.46	0.000
A × A	1	0.82310	0.823105	114.47	0.000
C × C	1	0.01919	0.019194	2.67	0.004
2-Way interaction	3	0.02479	0.024794	3.45	0.086
B × C	1	0.02479	0.024794	3.45	0.086
Error	13	0.09347	0.007190		
Lack- of- fit	8	0.05815	0.007269	1.03	0.612
Pure error	5	0.03532	0.007064		
Total	19	1.33410			

DF The total degrees of freedom are the amount of information in your data. The analysis uses that information to estimate the values of unknown population parameters. The total DF is determined by the number of observations in your sample. The DF for a term shows how much information that term uses. Increasing your sample size provides more information about the population, which increases the total DF. Increasing the number of terms in your model uses more information, which decreases the DF available to estimate the variability of the parameter estimates, *Adj SS* Adjusted sums of squares are measures of variation for different parts of the model, *Adj MS* Adjusted mean squares measure how much variation a term or a model explains, assuming that all other terms are in the model, *F value* is the test statistic used to determine whether any term in the model is associated with the response, including blocks and factor terms, *P value*. The *p* value is a probability that measures the evidence against the null hypothesis. Lower probabilities provide stronger evidence against the null hypothesis

3.2 2D Contour and 3D Surface Graphs for the Wear Behavior of CFRP Hybrid Nanocomposite

In this Section, 2D contour and 3D surface graphs have been used to demonstrate the dependence of the wear rate on the effectiveness of the parameters as design factors. Two of the factors should be varied while one of the factors should be held usually fixed or constant at zero level. Contours are drawn as a function of the two factors. These plots are useful for inspecting the effects of both, the interaction and main effects of factors on the wear rate.

3.2.1 Effect of Nanoclay and NanoZnO on Wear Rate

Figure 7a and b displays the 3-D contour and 2-D surface graphs for the nanoclay and the nanoZnO. The value of fiber orientation angle was considered fixed at zero level (45°). The contour graph shows that the value of the wear rate increased with an increase in the nanoclay wt% from coded design parameter level 0 to 1.6817 and gets decreased from − 1.6817 to 0 level wt% of the nanoclay. The effect of nanoZnO wt% has a combined effect of increase and decrease of the wear rate with the % variation of the nanoZnO. The combined effect of these two variables demonstrates a clear effect on the response at same time and also interaction between them shows significant effect on the wear rate. Similarly from the surface chart it can be understood on which surface value of nanoclay wt% and nanoZnO wt% one can get the lesser wear rate. The area under the curve can be treated as the measure of the wear resistance for the given conditions.

3.2.2 Effect of Nanoclay and Fiber Orientation on the Wear Rate

2D contour and 3D surface graphs for fiber angle of orientation and wt% of nanoclay are displayed in Fig. 8a and b correspondingly. The value of wt% for nanoZnO was held constant at the zero level (i.e., 3%). As seen in these plots, the amount of the wear rate increased generally with an increase in the level of fiber orientation angle; the wear rate decreases until 3% wt of nanoclay, after which it increases with wt% values of nanoclay. In addition, it is noticeable that by varying the value of the two variables affected, the wear rate at the same time is in increasing trend. Also, it shows the mutual interaction effect between the nanoclay and the fiber angle of orientation. Similarly from the surface chart it can be understood on which surface value of nanoclay wt% and fiber orientation angle one can get the lesser wear rate. The area under the curve can be treated as the measure of the wear resistance for the given conditions.

3.2.3 Effect of Fiber Orientation and NanoZnO on the Wear Rate

Figure 8a and b describes the 3-D contour and 2-D surface graphs between the fiber orientation angle and nanoZnO

Table 6 Regression coefficients and percentage of R^2 for both steps of analysis of variance for wear rate

Coefficients	b_0	b_1	b_2	b_3	b_{11}	b_{22}	b_{33}	b_{12}	b_{13}	b_{23}	R^2 %
Initial analyze	0.3198	0.1556	0.0262	0.0602	0.02413	0.0352	0.0398	0.0075	0.0328	0.0557	95.01
Final analyze	0.3486	0.1556	0.0262	0.02378	0.0363	–	0.0363	–	–	0.0557	92.99

b_0, b_1, b_2, b_3, b_{11}, b_{22}, b_{33}, b_{12}, b_{13}, b_{23} are the coefficients of regression equation

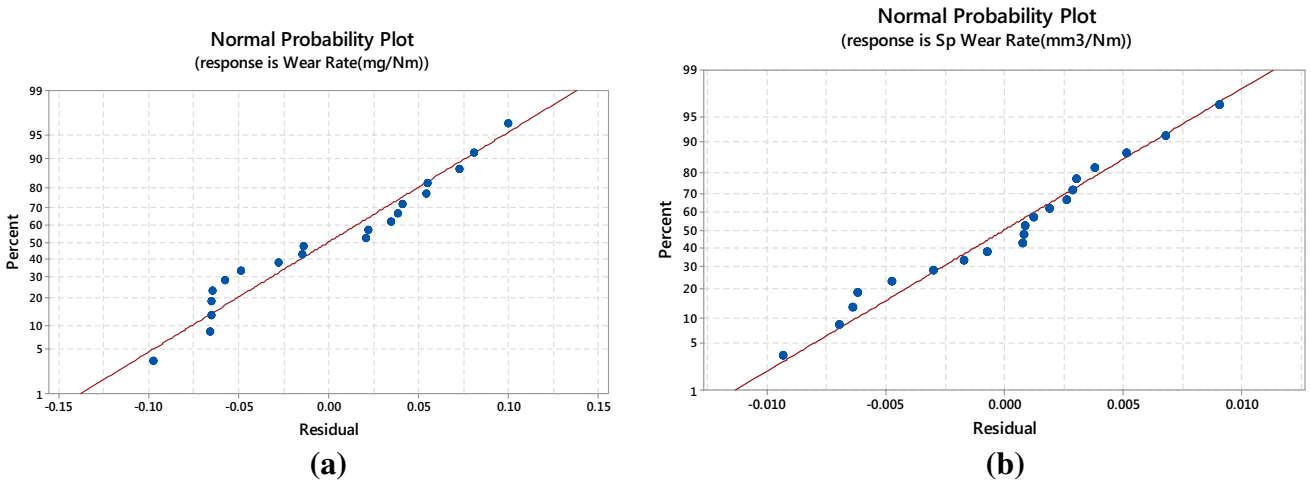

Fig. 4 Normal probability plots of residuals for **a** initial analysis, **b** final analysis of CFRP hybrid nanocomposites by RSM

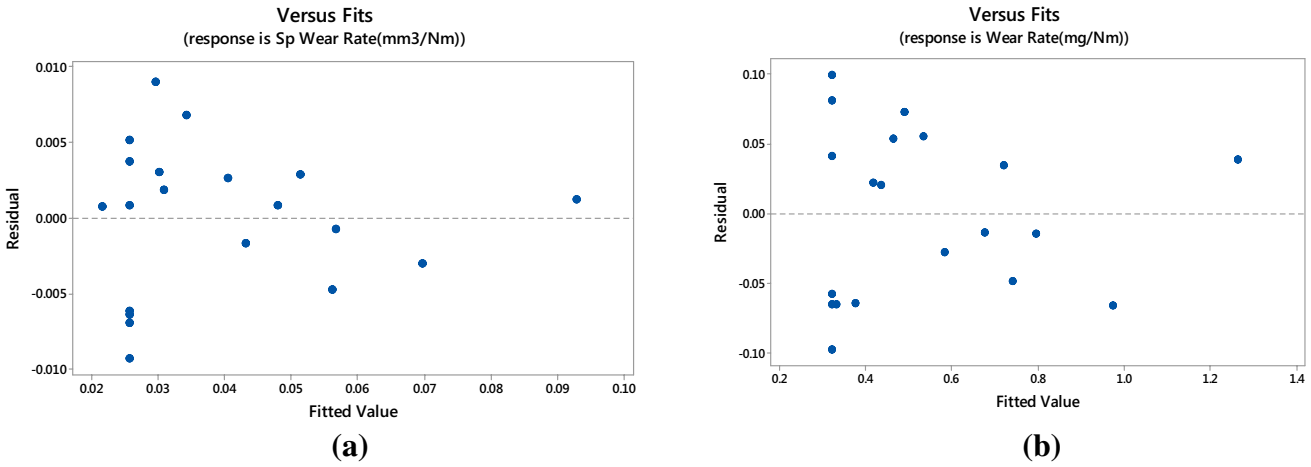

Fig. 5 Residual versus fitted values for **a** initial analysis, **b** Final analysis of CFRP hybrid nanocomposites by RSM

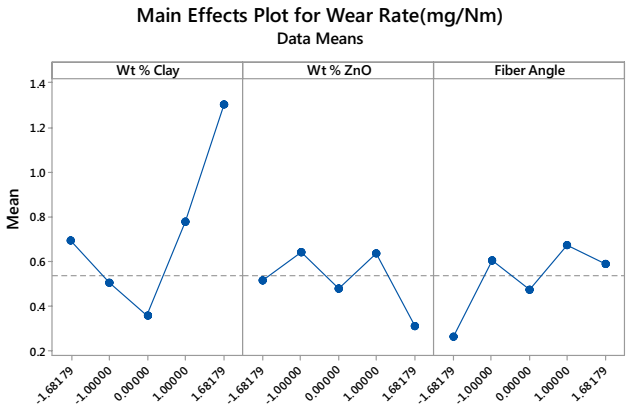

Fig. 6 Main Effects plot of for wear rate

and the nanoclay wt% was kept constant at zero level (3%). According to the surface and contour graphs, with an increase in the degree of the fiber angle of orientation, the wear rate decreases until 3% and then there is a slight increase in the wear rate. And the wt% nanoZnO increases the wear rate with its value. It can be seen from the contour graph that acceptable values of the wear rate can be obtained in the mid-portion of the values of fiber angle orientation and the wt% of nanoZnO displayed in the graph. Similarly from the surface chart it can be understood on which surface value of nanoZnO wt% and fiber orientation angle one can get the lesser wear rate. The area under the curve can be treated as the measure of the wear resistance for the given conditions.

The lowest value obtained for the wear rate was 2.22 mg/Nm which appeared in run no. 11 at coded levels nanoclay = 0, nanoZnO = 0, and fiber orientation angle = 0.

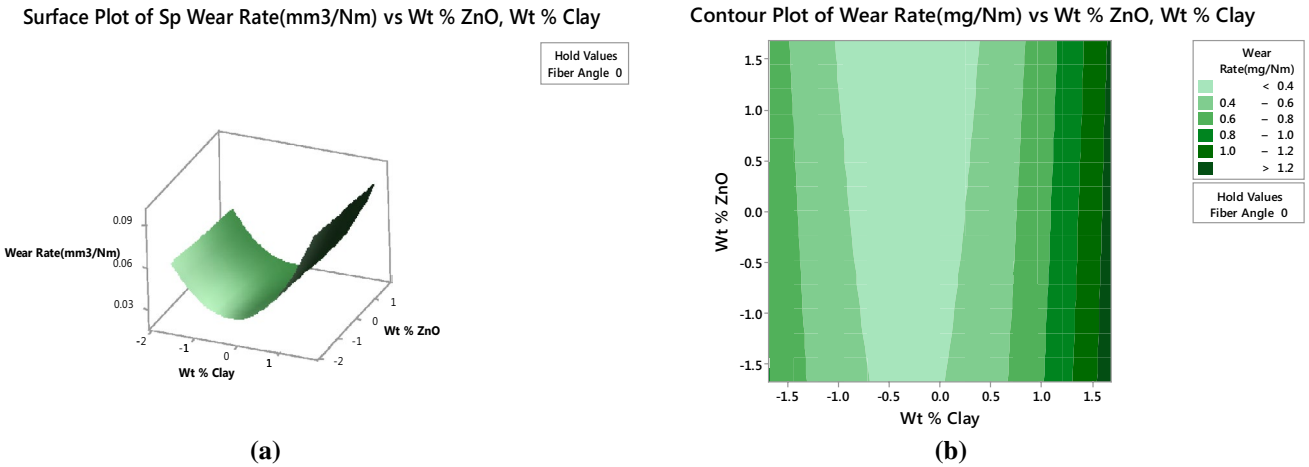

Fig. 7 **a** 3-D surface graph, **b** 2-D contour graphs, for effect of nanoclay and nanoZnO on wear rate

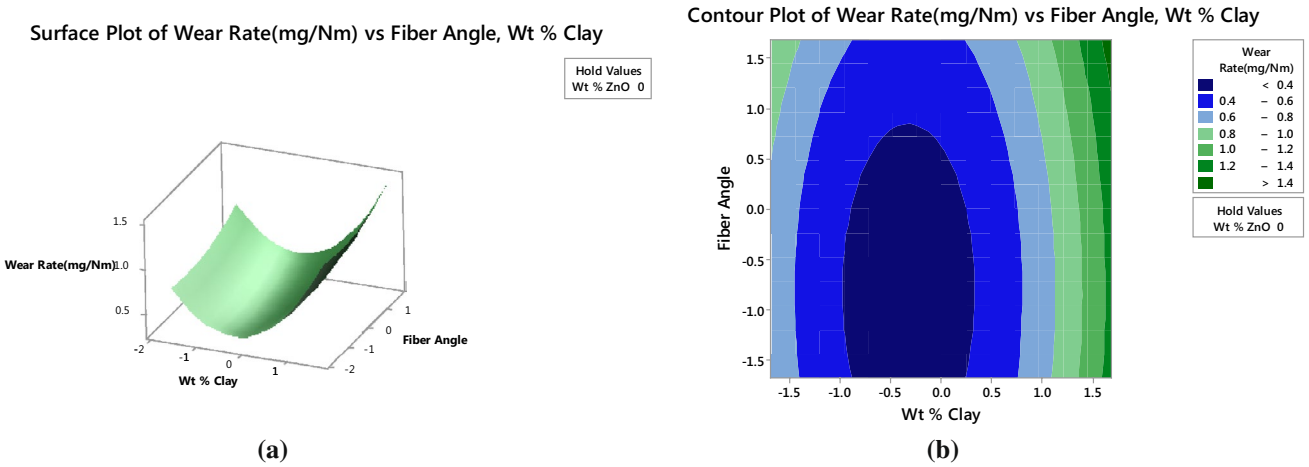

Fig. 8 **a** 3-D surface graph, **b** 2-D contour graphs, for the effect of nanoclay and Fiber angle on the wear rate

The respective actual values were nanoclay = 3%, nanoZnO = 3%, and fiber orientation angle = 45°, respectively.

3.3 Optimization of Wear Rate

In the optimization stage, the wear rate was calculated by using response optimizer in the Minitab software. For this, the minimum value for the wear rate was targeted up to 3.0 mg/Nm with nanoclay, nanoZnO, and fiber orientation values at 3 %wt, 2.9 %wt, and 9° correspondingly. By considering to these values for the fabricating the specimens, which is optimzed variables value based sample. These specimens are then tested for wear rate, the average value of wear rate is obtained as 4.2 mg/Nm.

3.4 SEM Analysis of Worn Surfaces of CFRP Hybrid Nanocomposites

Figure 9 shows the SEM morphologies of the worn samples of CFRP hybrid nanocomposites sliding against the steel pin and at room temperature, with and without nanoparticles, tested under different loading conditions. The exclusion of the fiber in the composite without nanoparticles was also very much infuriated with an increase in applied pressure as compared with the nano partcles filled composite, which proves the enhancement in wear resistance of the composites filled with nanoparticles. It is seen that most of the carbon fibers are pulled out from the fabric matrix on the worn surface. The surface was observed to be rough and showed obvious signs of scuffing of the unfilled carbon fabric composite (as shown in Fig. 10a), which indicates that the pure carbon fabric composite

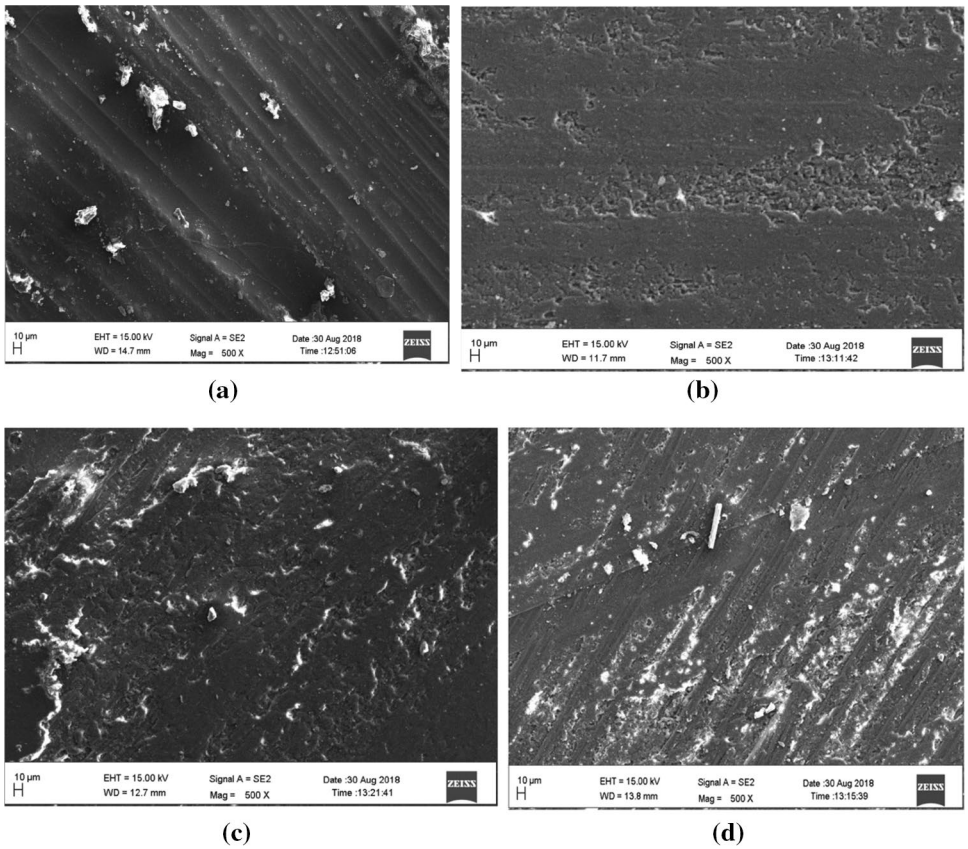

Fig. 9 SEM morphologies of the worn surfaces of carbon fabric composites reinforced with different fillers **a** pure CFC; **b** CF with nanoZnO 3% + nanoclay 3%; **c** CF with nanoZnO 4.2% + nanoclay 1.8%; **d** CF with nanoZnO 3% + nanoclay 5%

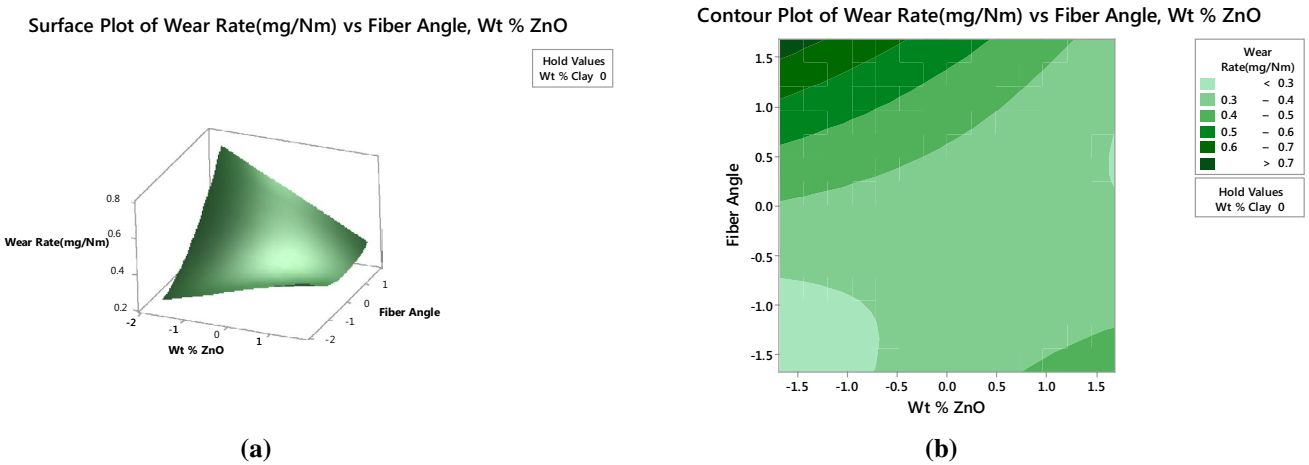

Fig. 10 **a** 3-D surface graph, **b** 2-D contour graph, for effect of nanoZnO and Fiber angle on wear rate

undertook a large contact stress and experiences severe peeling off as it slided against the steel at room temperature. Opposite to the above, the worn surface of the carbon fabric composite filled with nanoparticles is smooth and the pulling-out and exposure of the carbon fibers are nearly invisible (as shown in Fig. 10b) at coded level 11, having nanoclay 3 %wt and ZnO 3 %wt at fiber angle 45°.

This indicates that the nanoparticles included in the carbon fabric composite effectively act to increase the interface bonding strength between the carbon fiber and the adhesive resin, and hence to increase the mechanical strengths and wear resistance of the carbon fabric composites filled with nanoparticles. Moreover, the worn surface of the carbon fabric composite filled with wt 1.8% nanoclay and 4.2% wt nanoZnO at coded level 8 and with

wt 5% nanoclay and 3% wt of nanoZnO at coded level 1 is relatively smooth but still shows signs of carbon fiber pull-out, more rough and signs of scuffing (as shown in Fig. 10c and d), which agree well to the friction and wear behaviors of the composites filled with nanoZnO and nanoclay.

4 Conclusions

As in the studies of the past, it has been proved that the friction coefficient and wear rate can be significantly lowered with the application of nanoparticles [6–10]. In this study, the wear rate of the CFRP new hybrid nanocomposite material system has been investigated.

(1) The new material, i.e., CFRP hybrid nanocomposites with incorporation of nanoclay and nanoZnO can be used in carbon–carbon disc brakes, friction clutches, various parts of the space craft, aeroplanes, and automotive gear box which nowadays are being used in racing cars and in fabrication of automobile variable transmission systems from these CFRP hybrid nanocomposites.
(2) With the help of RSM and CCD design of experiments, one can find the optimum composition for wear rate.
(3) The Analysis of variance (ANNOVA) results shows that the nanoclay and nanoZnO had a direct, i.e., improved effect on wear properties with the 2–3% of the each nanoclay and nanoZnO, while the fiber orientation had an undesirable effect on minimizing the wear rate.
(4) The optimization result indicated that a minimum value for the wear rate from optimization given by the software was 3.0 mg/Nm. After manufacture and testing of the samples, the average value of the wear rate that was obtained was 4.2 mg/Nm which occurred in 2.9 wt% of nanoclay, 3 wt% of nanoZnO, and 0° of fiber angle of orientation. The optimization results also showed that the wear rate at the optimum value was much improved or minimized (about three times) than the controlled sample.
(5) The addition of or nanoZnO, and nanoclay with optimum quantity can contribute to increase the resistance of wear and friction-reducing capabilities of the carbon fabric composites. The carbon fabric composite filled with nanoclay 3 %wt and ZnO 3 % demonstrates the least friction coefficient and the smallest wear rate. The differences in the wear and friction properties of various nanoparticle-filled CFRP and pure CFRP composites are related to their respective interfacial interactions with the resin adhesive.

Acknowledgements The authors gratefully acknowledge the financial support of the R&D grant of the Mechanical Engineering Department, College of Engineering, Pune, (MS), India.

References

1. Wichmann MHG, Kopke U, Fiedler B, Schulte K (2004) Carbon nanotube-reinforced epoxy-composites: enhanced stiffness and fracture toughness at low nanotube content. Compos Sci Technol 64:2363–2371
2. Islam Md Ekramul, Tanjheel H et al (2015) Characterization of carbon fiber reinforced epoxy composites modified with nanoclay and carbon nanotubes. Proc Eng 105:821–828
3. Harishanand KS, Nagabhushana H et al (2013) Comparative study on mechanical properties of ZnO, ZrO_2 and CeO_2 nanometal oxides reinforced epoxy composites. Adv Polym Sci Technol 3(1):7–13
4. Deka Biplab K, Maji Tarun K (2012) Effect of nanoclay and ZnO on the physical and chemical properties of wood polymer nanocomposite. J Appl Polym Sci 124:2919–2929
5. Rashmi NM, Renukappa B (2011) Suresha, Dry sliding wear behaviour of organo-modified montmorillonite filled epoxy nanocomposites using Taguchi' s techniques. Mater Des 32:4528–4536
6. Chang Li, Friedrich Klaus (2010) Enhancement effect of nanoparticles on the sliding wear of short fiber-reinforced polymer composites: a critical discussion of wear mechanisms. Tribol Int 43:2355–2364
7. Shazed MA, Suraya AR, Rahmanian S, Mohd Salleh MA (2014) Effect of fibre coating and geometry on the tensile properties of hybrid carbon nanotube coated carbon fibre reinforced composite. Mater Des 54:660–669
8. Hawkins Jr David A, Anwarul A (2014) Fracture toughness of carbon-graphene/epoxy hybrid nan ocomposites. Proc Eng 90:176–181
9. Boroujeni AY, Al-Haik M, Emami A (2017) R Kalhor (2017) Hybrid ZnO nanorod grafted carbon fiber reinforced polymer composites; randomly versus radially aligned long ZnO nanorods growth. J Nanosci Nanotechnol 18(6):4182–4188
10. Ayyagari Suma, Al-Haik Marwan, Rolli Virginie (2018) Mechanical and electrical characterization of carbon fiber/bucky paper/zinc oxide hybrid composites. J Carbon Res C 4:6. https://doi.org/10.3390/c4010006,1-18
11. Naga Raju B, Ramji K, Prasad VSRK (2015) Mechanical properties of glass fiber reinforced polyester ZnO nano composites. Mater Today 2:2817–2825
12. Kong K, Deka BK, Kwak SK, Oh A, Kim H, Park YB, Park HW (2013) Processing and mechanical characterization of ZnO/polyester woven carbon–fiber composites with different ZnO concentrations. Compos Part A 55:152–160
13. Rajasekhar P, Ganesan G, Senthilkumar C (2014) Studies on tribological behavior of polyamide filled jute fiber- nano-ZnO hybrid composites. Proc Eng 97:2099–2109
14. Alipour Skandani A, Masghouni N et al (2012) Enhanced vibration damping of carbon fibers-ZnO nanorods hybrid composites. Appl Phys Lett 101:073111
15. Guo Chuangqi, Zheng Zhen, Zhu Qiren, Wang Xinling (2007) Preparation and characterization of polyurethane/ZnO nanoparticle composites. Polym Plast Technol Eng 46:1161–1166
16. Rostamiyan Y, Fereidoon A et al (2015) Using response surface methodology for modeling and optimizing tensile and impact strength properties of fiber orientated quaternary hybrid nano composite. Compos B 69:304–316
17. Rostamiyan Y, Fereidoon A et al (2015) Experimental and optimizing flexural strength of epoxy-based nanocomposite: effect of

using nano silica and nano clay by using response surface design methodology. Mater Des 69:96–104
18. Tripathi VK, Kulkarni NS (2014) OptiComp: a comprehensive procedure for optimal design of a composite laminate. Int J Eng Sci 8(2):110–120
19. V. K. Tripathi, M. J. Sable, S. S. Sonawane, K.V. Nemade, U. V. Hambire (2013) Optimum design of systems using principles of optimization, In Handbook of 7th Asian Conference on Fixed Point Theory and Optimization, University of Kasetsart, Thailand
20. Sanes J, Carrión FJ, Bermúdez MD (2010) Effect of the addition of room temperature ionic liquid and ZnO nanoparticles on the wear and scratch resistance of epoxy resin. Wear 268:1295–1302
21. Bahadur S, Sunkara C (2005) Effect of transfer film structure, composition and bonding on the tribological behavior of polyphenylene sulfide filled with nano particles of TiO_2, ZnO, CuO and SiC. Wear 258:1411–1421
22. Kang Yingke, Chenb Xinhua et al (2012) Friction and wear behavior of nanosilica-filled epoxy resin composite coatings. Appl Surf Sci 258:6384–6390
23. Yan L, Wang H, Wang C et al (2013) Friction and wear properties of aligned carbon nanotubes reinforced epoxy composites under water lubricated condition. Wear 308:105–112
24. Zhang Xin-Rui, Pei Xian-Qiang et al (2009) Friction and wear studies of polyimide composites filled with short carbon fibers and graphite and micro SiO_2. Mater Des 30:4414–4420
25. Ramachandra M, Abhishek A et al (2015) Hardness and wear resistance of ZrO_2 nano particle reinforced al nanocomposites produced by powder metallurgy. Proc Mater Sci 10:212–219
26. Mallakpour S, Behranvand V (2016) Nanocomposites based on biosafe nano ZnO and different polymeric matrixes for antibacterial, optical, thermal and mechanical applications. Eur Polym J. https://doi.org/10.1016/j.eurpolymj.2016.09.028
27. Zhang G, Sebastian R (2012) Role of monodispersed nanoparticles on the tribological behavior of conventional epoxy composites filled with carbon fibers and graphite lubricants. Wear 292–293:176–187
28. Sudeepan J, Kumar K et al (2014) Study of friction and wear of ABS/Zno polymer composite using taguchi technique. Proc Mater Sci 6:391–400
29. Zhang Zhao-Zhu, Feng-Hua Su et al (2005) Study on the friction and wear properties of carbon fabric composites reinforced with micro- and nano-particles. Mater Sci Eng A 404:251–258
30. Senthil Kumar MS, Mohana Sundara Raju N (2015) Tribological analysis of nano clay/epoxy/glass fiber by using Taguchi's technique. Mater Des 70:1–9
31. Molazemhosseini A, Tourani H (2013) Tribological performance of PEEK based hybrid composites reinforced with short carbon fibers and nano-silica. Wear 303:397–404
32. Kalin M, Zalaznik M et al (2015) Wear and friction behavior of poly-ether-ether-ketone (PEEK) filled with graphene, WS2 and CNT nanoparticles. Wear 332–333:855–862
33. Abdullahi U, Maleque MA (2013) Wear mechanisms map of CNT-Al nano-composite. Proc Eng 68:736–742
34. Sangeetha M, Prakash S (2015) Wear properties estimation and characterization of coated ceramics with multiwall carbon nano tubes (MWCNT) reinforced in aluminium matrix compositesFRP composites. J Tribol 6:24–36
35. Ambekar SD, Tripathi VK (2019) Optimization of flexural strength of CFRP hybrid nano composites containing nanoZnO and nanoclay particles. Int J Interact Des Manuf. https://doi.org/10.1007/s12008-019-00539-w
36. Zhou K et al (2011) Size prediction of particles caused by chipping wear of hard coatings. Wear 271(7–8):1203–1206
37. Liu B, Zhou K (2019) Recent progress on graphene-analogous 2D nano materials: properties, modeling and applications. Prog Mater Sci 100:99–169
38. Wang Y et al (2019) Effects of tensile strain rate and grain size on the mechanical properties of nano crystalline T-carbon. Comput Mater Sci 170:1–8